Diffractive Optical Propagation Techniques for Mixed-Signal CAD Tools

Timothy P. Kurzweg[a], Steven P. Levitan[*a], Jose A. Martinez[a], Philippe J. Marchand[b], Donald M. Chiarulli[c]

[a]Department of Electrical Engineering, University of Pittsburgh

[b]Optical Micro Machines, San Diego, CA 92121

[c]Department of Computer Science, University of Pittsburgh

ABSTRACT

Computer Aided Design (CAD) tools for modeling optical computing systems use a variety of different optical propagation techniques. However, for modeling micro-systems, common optical modeling techniques are not always valid. This paper discusses various optical propagation models for optical micro-systems by examining the requirements imposed by the physical size of the microsystems and the goal of achieving an interactive CAD framework. Based on these constraints, an appropriate optical model is chosen and used in our opto-electro-mechanical CAD tool, Chatoyant, to perform simulations of 2x2 micro-optical switch systems.

Keywords: MEMS-CAD, optical MEMS, MOEMS, OMEMS, micro-optics, optical propagation

1. INTRODUCTION

High-speed optical switching systems based on optical micro-electrical-mechanical (OMEM) devices are a critical backbone technology for next generation computer networks and systems. These devices are capable of switching multiple optical channels using fiber ribbon cable as the input and output medium, and free space optics in the switching component. OMEM devices are used to implement the switch function using techniques such as physically deflecting each beam based on the electrostatic displacement of a microscopic mirror. Systems built with these switches have numerous advantages over typical waveguide or fiber switching systems, including the reduction of coupling loss and crosstalk, and being independent of wavelength, polarization, and data format[21]. The switches have been reported to be 10 times smaller and faster than typical fiber-based switches, while requiring only 1/100th of the operating power[16]. Systems built with these switches have increased system reliability and reduced system costs. However, like many new technologies, design methods and tools for these systems are currently ad-hoc. Designers typically use combinations of tools that were built for the individual domains of optics, mechanics and electronics with little integration and with system level analysis based only on the experience of the designer or simply on assumptions about the ensemble behavior of the components.

In order to support the design of these switching systems in a practical manor, computer aided design tools must be capable of modeling, electronics, electrostatics, mechanics, guided wave optics, and free space optics. The design tools must directly support the interfaces between models in all these domains, and characterize the behavior of the resulting system in an interactive environment. Obviously, CAD tools exist in each of these domains and we have no intention of re-inventing these tools. For example, CAD tools for conventional MEMS are being designed in both academia and industry, including those by CMU[15], Microcosm[14], and MEMScap[13]. These tools typically perform a finite element (FE) simulation of MEM components, and many have extensions to a system-level evaluation of electronics and mechanics. However, these tools do not provide a single multi-domain design environment.

Our interest is in modeling system behavior in a single integrated framework. This is what we have achieved in our free-space opto-electro-mechanical CAD tool, Chatoyant[7,9]. Chatoyant is built upon Berkeley's object-oriented simulation engine Ptolemy[3]. Chatoyant's component models are written in C++ with sets of user defined parameters for the characteristics of each module instance. Chatoyant performs static simulations to analyze such effects as mechanical tolerancing, power loss, insertion loss, and crosstalk, while dynamic simulations analyze data streams with techniques such as noise analysis and BER calculation.

* Correspondence: Email: steve@ee.pitt.edu; WWW: http://kona.ee.pitt.edu/pittcad; Telephone: 412 648 9663; Fax: 412 624 8003

This paper examines optical propagation techniques, appropriate for modeling optical MEM systems. We first define the requirements for a system-level optical MEM CAD tool and examine typical MEM systems, determining the requirements established by the physical properties of these components and systems. Next, we examine the possible free-space optical propagation techniques that can be used for modeling OMEM systems. These techniques are compared in terms of their validity and effectiveness in achieving our goals for system-level CAD tools. This is followed by a short discussion of some of the optical components we have modeled utilizing scalar optical propagation methods. We conclude by presenting results from modeling an optical crossconnect (OXC) switch in Chatoyant.

2. SYSTEM CONCERNS

As stated above, our goal is to create a system-level CAD tool for the interactive design of optical MEM systems. Therefore, we are not only striving for accuracy, but we also require fast algorithms, producing simulation results in a reasonable time. Additionally, a system level tool needs to evaluate such system concerns as BER (bit error rate), insertion loss, and crosstalk. Therefore, the model for light propagation must support optical power information, such as intensity, phase, and frequency (wavelength) dependence. To further identify the appropriate optical modeling technique, we must examine typical optical MEM systems and evaluate the available optical propagation techniques which satisfy the requirements imposed by these systems.

As an example of an optical MEM system, we examine Lin et al.'s micromachined switch[11]. A graphical drawing of this 8x8 OXC is seen in Figure 1. The eight input fibers to be switched come from the left side. This system implements a true crossbar switch, where each input can be routed to any of the output fibers, lined across the bottom of the chip. In order to make every connection available, there are 64 hinged mirrors lying on the surface of the chip. As an interconnection is desired, the specified mirror that can complete the interconnect is "lifted" off the surface, using conventional MEM components such as scratch drive actuators (SDA), into a standing position with a 45 degree angle relative to the incoming light. In the figure, two example interconnects are completed, the black mirrors represent mirrors that are standing and the grey mirrors represent mirrors that remain lying down. This system has a switching speed of less than 700 μsec with negligible crosstalk and is polarization independent. By using this system as a representative OMEM application, we can determine the type of optical modeling that is required for modeling mixed-signal micro-systems.

The collimating lenses seen in Figure 1 could be either refractive or diffractive elements. Typically in these switches, the lenses are diffractive micro-Fresnel lenses due to their ease of fabrication. However, these lenses are inefficient and greatly increase the optical insertion loss. Therefore, in some systems, refractive lenses or fiber collimators are being considered. The use of both diffractive and refractive components require the use of diffractive optical models for complete system modeling.

The sizes of the components and the propagation distances between the components also constrain the optical propagation model. For example, the mirrors in this switch have dimensions of 150x140 μm. Sizes in other optical MEM components can shrink further, as seen in Texas Instruments's DMD (digital micromirror device) chips, where the 500,000 mirrors on the chip are each only 16 μm[6]. Since OMEMS are fabricated with the same techniques as electronic VLSI design, the size of a

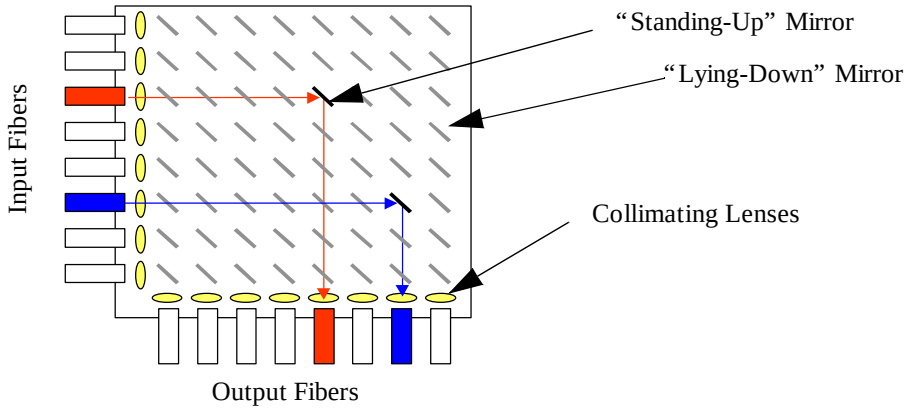

Figure 1: Free-Space Micromachined Optical Switch[11]

OMEMS chip does not exceed a couple of millimeters, therefore, typical distances between components (i.e., propagation distances) are approximately 10-1000 μm. For example, the pitch between the mirrors in Figure 1 is 500 μm. With the sizes and distances on the order of only ten to a thousand times the wavelength of light, optical diffractive models are required even for applications composed of purely refractive components.

The last requirement illustrated by examining the switch is that the optical models must easily interface with fiber-based CAD tools. This is seen by the light coming "on-" and "off-" chip through fibers. Currently, there is no need to build new models for fiber propagation, since it is being done with the beam propagation method (BPM) and/or the finite difference (FD) modeling in such commercial tools as RSoft's BeamPROP[18] and Optiwave's BPMCAD[17].

We next examine some of the common optical propagation techniques with respect to modeling OMEM systems. Summarizing our study of the OMEM systems and the goals for an interactive CAD tool, we require an optical propagation technique that is computationally fast, supports diffractive effects, and is valid for the small sizes and propagation distances of the optical MEM components and systems.

3. OPTICAL PROPAGATION TECHNIQUES

Ray, or geometric, optics are the simplest of the optical propagation methods. This method traces rays of light through refractive elements, however has no inherent support for the optical characteristics of light. This is improved by using Gaussian optics, which satisfies the paraxial Helmholtz equation in solving for optical parameters such as waist size, depth of focus, intensity, and phase, meeting the optical criteria which is required for modeling optical MEM systems. An additional benefit of using Gaussian analysis is that we can approximate the behavior of the lasers used in these systems as sources of Gaussian shaped beams. The greatest advantage of both these methods is speed. Using nine scalar parameters to define a Gaussian beam and the ABCD matrix equations for optical interfaces, no explicit integration is needed to calculate the resulting Gaussian beam at the interface to adjacent components[19]. Therefore, the computational complexity for both Gaussian and ray optic models is on the order of the number of beams that are being propagated. Chatoyant's support for macro-systems is based on the Gaussian modeling technique[10]. However, as we have illustrated with the switch example above, modeling optical diffraction is a requirement for simulating optical MEM systems. Therefore we need to consider appropriate optical propagation methods which can meet this objective without sacrificing simulation speed.

Figure 2 is a tree that begins at the top with Maxwell's equations and branches downward through the different abstraction levels of scalar modeling techniques. Along the arrows, notes are added stating the limitations and approximations that are made to get to the next, less accurate model.

All scalar diffraction solutions are limited by two assumptions; the diffracting structures must be "large" compared with the wavelength of the light and the observation screen can not be "too close" to the diffracting structure. The concept of "too close" is defined for each approximation model in Figure 3. This figure shows light passing through an aperture plane (ξ,η), propagating a distance z past the aperture, and striking an observation plane (x,y). The figure also presents equations calculating the validity of the diffractive models with respect to the distance propagated past the aperture, in terms of the limits of the aperture and observation planes, the wavelength of light, λ, and the wave number, $k=2\pi/\lambda$.

Working from the bottom to top of Figure 2 and from right to left of Figure 3, we first investigate the least accurate of the scalar approximations, the Fraunhofer approximation. The advantage of this technique is the ability to implement a Fourier transform to solve the complex wave function. The Fraunhofer technique is valid when the light striking the aperture plane can be assumed to be a plane wave[2]. Most diffractive software tools perform Fraunhofer propagation, using a common FFT routine for quick evaluation. As shown in Figure 3, the Fraunhofer approximation is valid in the "far-field", where the light has propagated to a distance far from the aperture, and the diffraction pattern is essentially the same as that at infinity. However, for most optical MEM systems, the far field is not of concern. To illustrate the problem of this method with respect to typical micro-optical systems, we consider a system with an aperture of 50 μm and an observation plane of 200μm, using a 850 nm light source. Using the equation found in Figure 3, the minimum propagation distance for the Fraunhofer approximation to be valid is 4.6 mm, over 5 times the propagation pitch found in the switch example.

To remove the plane-wave limitation of the far-field, our study moves up the tree, towards more rigorous optical models. We

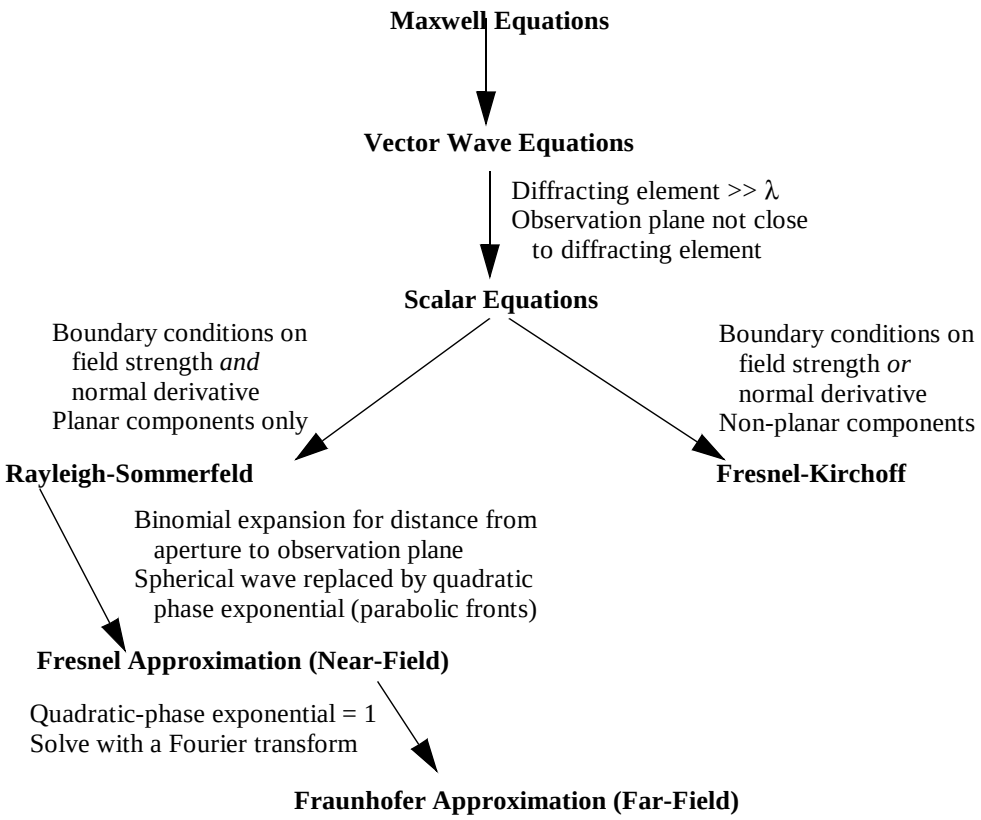

Figure 2: Diffractive Modeling Techniques

next examine the Fresnel approximation, valid in both the far and near field. The "near field" is defined as the region closer to an aperture where the diffraction pattern differs from that observed at an infinite distance. No longer can a fast Fourier transform be used for this calculation, as the light hitting the aperture plane is no longer a plane wave and an explicit integration of the wave front must be calculated. When solving for the minimum propagation distance for validity with the same example system as before, we find the propagated distance must be larger than 966 μm, approximately twice the propagation distances found in the switch example, making this method also invalid for many optical MEM systems. Therefore, our search for an appropriate optical propagation method continues in order to support propagation distances smaller than the near field limit.

We next examine more rigorous scalar diffraction models, the Fresnel-Kirchoff and Rayleigh-Sommerfeld scalar formulations. Both of these methods produce similar, accurate results, again with the use of an explicit integration of the complex wavefront. The difference between the two methods lie in their handling of the boundary conditions. Fresnel-Kirchoff has boundary conditions on both the field strength and normal derivative, whereas the Rayleigh-Sommerfeld removes this incon-

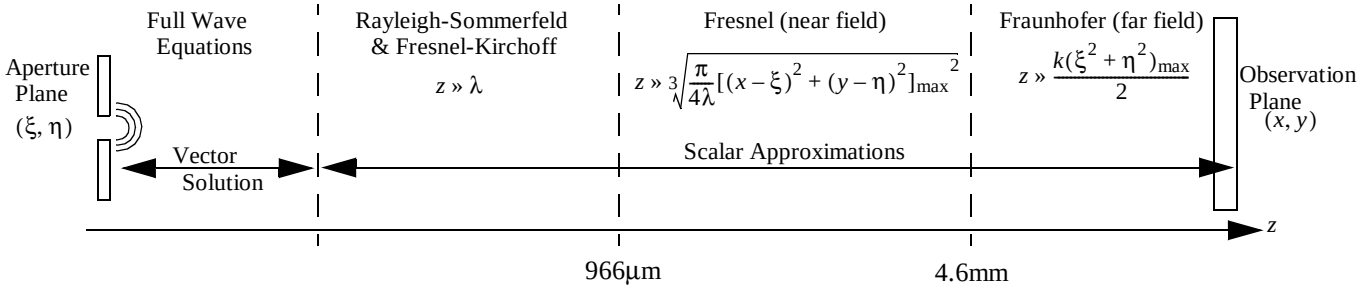

Figure 3: Optical Propagation Distance, *z*, Aperture Size, *(ξ,η)*, Observation Plane Size, *(x,y)*, and Model Validity

sistency and imposes boundary conditions on either the field strength or the normal derivative, since they are related. Unlike the Fresnel-Kirchoff formulation, the Rayleigh-Sommerfeld is limited to planar components. However, for small angles, these methods are identical. These formulations are only limited by the propagation distance being "greater" than the wavelength of light. Therefore, with valid diffractive ranges and required optical characteristics, we believe that these formulations are the appropriate optical propagation methods to use for the modeling and simulation of current optical MEM systems. However, we must evaluate their computation efficiency to ensure our system-level CAD requirements are also satisfied.

We have chosen to use the Rayleigh-Sommerfeld equation over the Fresnel-Kirchoff due to simplicity in the equation form[4]. For this formulation, we see the required integration has the form:

$$U(x,y) = \frac{z}{j\lambda}\iint_{\Sigma} U(\xi,\eta)\frac{e^{jkr}}{r}d\xi d\eta \quad ,$$

where, k is $2\pi/\lambda$, r is the distance from the source point (ξ,η) to the observation point (x,y), z is the distance propagated, Σ is the area of the aperture, and U is the complex optical wave function. This equation mathematically describes the Huygens-Fresnel principle in rectangular coordinates, where each point on the aperture plane is a source of spherical waves[5]. This results in the requirement that U for each point in the observation plane be calculated through the superposition of all the input sources.

The computation time of this scalar technique is therefore based on the gridding of both the aperture and observation plane. For each grid point in the observation plane, $U(x,y)$, a double integration is performed over every grid point in the aperture plane, $U(\xi,\eta)$. This is costly in computation time, however, several optimizations can be performed. First, computation time can be saved by decreasing the number of grid points used to represent the complex wave function, at a cost of accuracy. Second, in systems with radial symmetry, the integration can be reduced to a single integral. Finally, the integration algorithm chosen factors largely in the computation time.

We use a 2-dimensional application of the Gaussian quadrature technique with order N=96 to perform the integration in the Rayleigh-Sommerfeld equation[1]. In this technique, the aperture plane is divided into NxN predefined segments, each associated with a unique weight. The estimate for the integration solution of a point in the observation plane is a linear summation of the propagating complex wave function, produced by the individual points of the aperture plane multiplied by the corresponding weights of the quadrature approximation.

We have found this Gaussian quadrature integration method to be both accurate and efficient for solving the Rayleigh-Sommerfeld integration. It is well known that quadrature integration techniques offer the optimum estimate of the exact integration solution for the chosen number of points (N). However, the accuracy of this method is dependent of the smoothness of the integrated function, since the function is effectively interpolated by a polynomial of degree 2N+1. In the Rayleigh-Sommerfeld expression, the possible causes of high order (i.e., "non-smooth") effects are found at the interactions of the complex wave function at the finite boundaries of the apertures. The Gaussian quadrature method will result in an accurate solution if the discontinuities in the wave function at the boundaries are negligible. This condition is satisfied by the Rayleigh-Sommerfeld initial assumption that the aperture size is larger that the wavelength of the light.

In Figure 4, we show Chatoyant's Rayleigh-Sommerfeld simulation results of the 850 nm plane wave, 50 μm aperture, and 200 μm observation plane example that we examined earlier. We compare our simulations with a 80x80 grid-point "base case" from MathCAD, which uses a Romberg integration technique. The table in Figure 4 shows the computation time and relative error of the system (compared with the base case) for different grid spacing. We can see that the simulation that takes 2 hours using a Romberg algorithm can be reduced to approximately 4.5 minutes using our optimized Gaussian quadrature integration technique. The relative RMS error of this method compared to the base case is only 0.6%. As can be seen, the user can choose to reduce Chatoyant's simulation time even further at a cost of accuracy in the result.

4. OPTICAL COMPONENT MODELING

Our diffractive optical components in Chatoyant include apertures, screens, lenses, computer generated holograms, and plane mirrors. As seen above, we use a rectangular coordinate system to define each aperture and observation plane. Apertures are the simplest to model. As the light propagates to the aperture, the complex wave function is calculated over the entire obser-

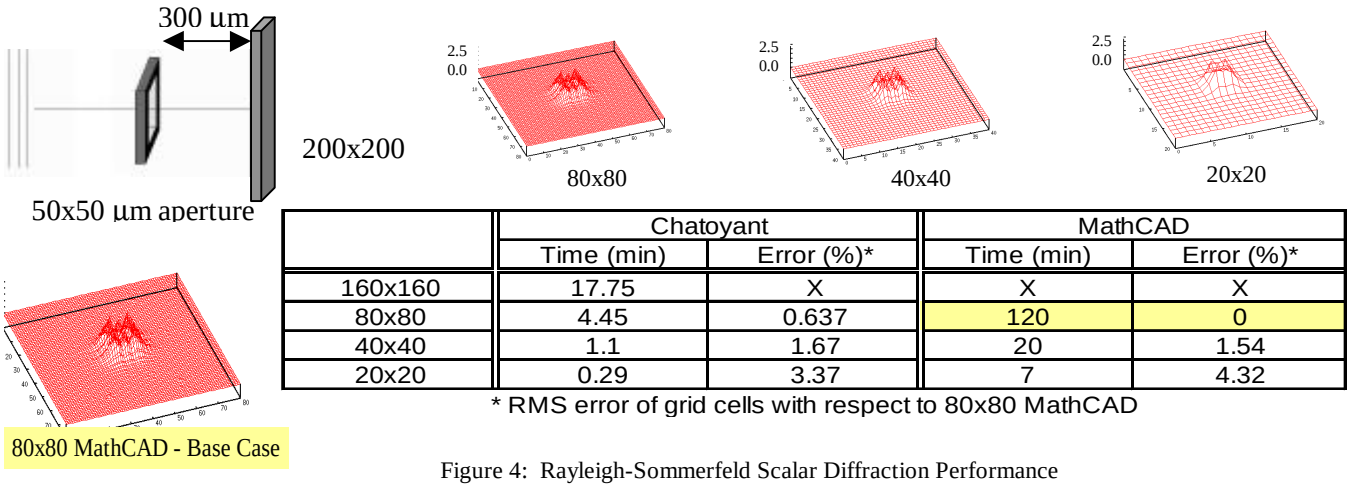

	Chatoyant		MathCAD	
	Time (min)	Error (%)*	Time (min)	Error (%)*
160x160	17.75	X	X	X
80x80	4.45	0.637	120	0
40x40	1.1	1.67	20	1.54
20x20	0.29	3.37	7	4.32

* RMS error of grid cells with respect to 80x80 MathCAD

Figure 4: Rayleigh-Sommerfeld Scalar Diffraction Performance

vation plane. To account for the aperture, an "on/off" mask is multiplied by the complex function, passing the light through the aperture and blocking the light that does not pass through, by multiplying by 1 and 0, respectively. The shape of the mask can be arbitrary, as long as it can be defined by the rectangular grid points. For example, a circular aperture is composed by checking if the coordinates of each square grid point are within the radius of the circle. Optical screens simply invert the "on/off" mask, blocking the center of the aperture and letting the rest of the light pass.

Refractive lenses act as a phase transformation, resulting when optical beams propagate through different indices of refraction. To model refractive lenses, we confine the lens' phase function with an aperture, usually circular. The phase function of a refractive thin lens, p_{tl}, is dependent on the lens' focal length, f, and wave number, $k = \frac{2\pi}{\lambda}$. We note that even refractive lenses produce diffractive effects when the beam is clipped. The phase function is:

$$p_{tl}(x,y) = e^{-j\frac{k}{2f}(x^2+y^2)}$$

A Fresnel lens is designed to change both the light's intensity and phase, causing the light to interfere and form a focused spot. This lens is composed of bands of material that allow or restrict the propagation of the complex light wave. These diffracting rings affect the light wave such that the pattern acts as a spherical lens with an exact focal length. However, in practice, the efficiency of these lenses is limited to approximately 10% for micro-optical systems. To simulate the lens, the transmission property of the rings are multiplied by the complex wave function. This transmission property can be thought of as a 0 (opaque band) or 1 (transparent band) phase function, as found in:[19]

$$p_{fl}(x,y) = \begin{cases} 1, \text{ if } \cos\left(\pi\frac{x^2+y^2}{\lambda f}\right) > 0 \\ 0, \text{ otherwise} \end{cases}$$

The propagation of light through a computer generated hologram (CGH) is another diffractive effect that we model. CGHs often are used to create a desired beam pattern, for example, creating a spot array. Holograms are created by etching the holographic material (usually glass or plastic) to different thicknesses, creating a phase mask. As the light propagates through the diffractive phase mask, it reconstructs the original holographic pattern.

When modeling reflection off a mirrored surface, we start by performing the same aperture routine as seen above, defining the wavefront that strikes the mirror. This mirror "aperture" is again the source for the next component, however, instead of the light refracting through the surface, these wavefronts are reflected off the mirror. Besides the fundamental phase change of the light, no essential change to the Rayleigh-Sommerfeld equation is necessary[2].

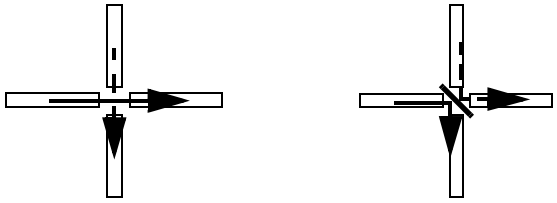

Figure 5: 2x2 Optical MEM Switch

5. SIMULATION OF 2X2 OPTICAL MEM SWITCH

In the next section, we simulate and analyze an optical MEM switching system. The system is a 2x2 switch, similar to those being built by Bell-labs[20], UCLA[8], and University of Neuchael, Switzerland[12]. All these switches are based on the same 2x2 switching architecture, seen in Figure 5. This consists of a set of four fibers in the shape of a "+" sign. The switch is in the "cross" state when light is passed straight across the gap. However, to achieve the "bar" state, a mirror is inserted between the fibers at a 45 degree angle, and the light is reflected to the alternate output.

Examining only the cross state of the switch, we simulate this system with the addition of collimating lenses. In theory, this optical system should focus the light back onto the output fiber, with the same waist size and intensity. In this simulation, the focusing system uses two 100 µm diameter lenses (focal length of 50 µm) separated by 100 µm. The first lens is placed 50 µm from the input fiber, and the second lens is 50 µm before the output fiber. The configuration can be seen in Figure 6. BeamPROP is used and interfaced with Chatoyant to model the propagation through the fibers. The interface between the programs is a data file containing the gridded complex wave function. The fibers are both 10 µm core, single mode fibers with an core/cladding index difference of 0.006, length of 1000 µm, and optimized for 1550 nm wavelength light. A 1550nm Gaussian

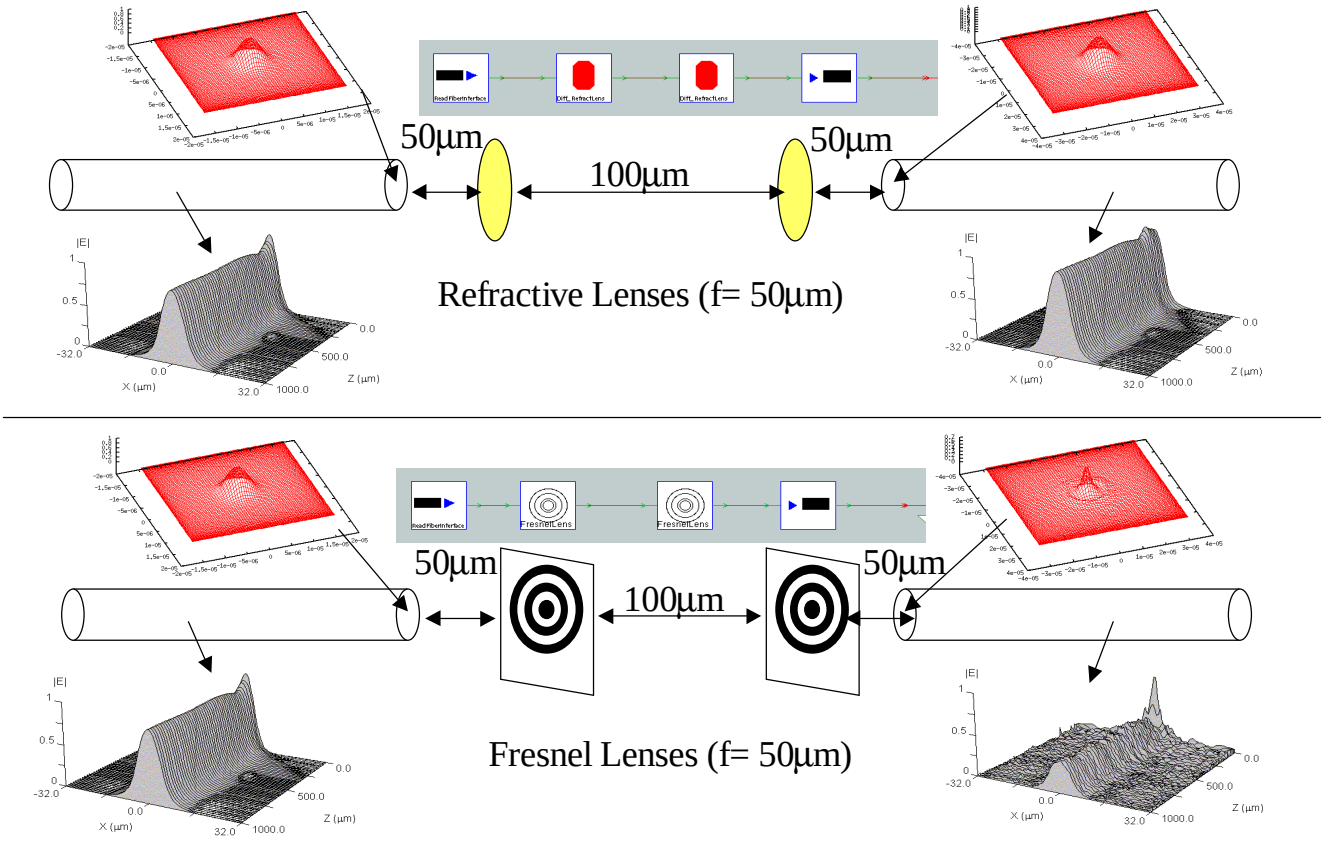

Figure 6: Lens comparison in the Cross state

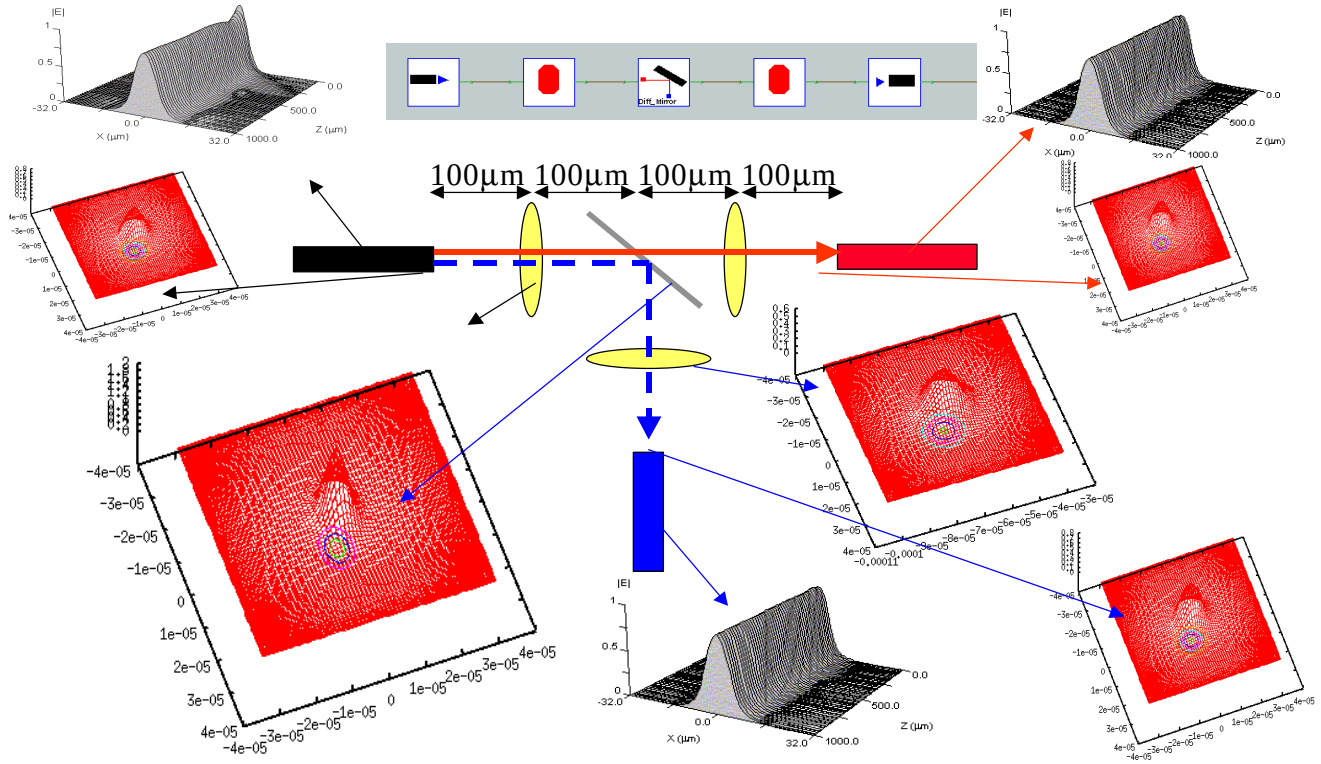

Figure 7: Switch Simulation

beam with a 10 µm waist is used as a source to the first fiber. This input is close to the ideal "mode" of the fiber.

Two different simulations are shown in Figure 6. The first uses refractive lenses, and the second uses diffractive binary Fresnel lenses. The Chatoyant sub-system is shown above the fibers, containing the four components of the focusing system: the fiber/free-space interface, two lenses, and the free-space/fiber interface. At each interface Chatoyant displays the intensity of the light. In the simulation using the refractive lenses, the light is focused well onto the out-going fiber, resulting in the wave quickly being captured back into the core of the fiber. However, when using the Fresnel lenses, it can be seen from the Chatoyant's output intensity wave, shown in Figure 6, that these lenses did not focus the beam of light well on the front of the second fiber. This results in some of the power being lost through the cladding as the beam propagates down the fiber. The poor focusing is a result of the difficulty in creating a binary Fresnel lens with a focal length of 50 µm. Multi-level phase lenses could be used to accurately focus the beam in the required 50 µm, however at a cost of fabrication complexity.

The next example shows the switch working in both the bar and cross states. Refractive lenses (f = 100 µm) were used. The system set-up and simulation results for both switching states are seen in Figure 7 Again, Chatoyant intensity outputs are seen at each component throughout the system. If no mirror is present, the light propagates straight through and achieves a cross connection, as shown by "solid" arrow. However, with the addition of the mirror, the optical path is reflected 90 degrees, as shown by the "dashed" arrow, and the bar state is connected. In these simulations, the mirror model is assumed to be ideal, with a 100% reflectivity. The additional arrows in the figure match the intensity distributions to the component surfaces. As the light propagates through free-space, one can see how the beam waist expands. Also notice, how the beam appears oval on the tilted 45 degree mirror intensity output. Both the cross and the bar states have less than 1dB of loss through the free-space switching system, and are accepted into output fiber.

For both of these simulations of the switch, each free-space propagation took approximately two minutes of computation time, running on a 500MHz Pentium III machine running Linux. Therefore, with the mirror in the bar state, the simulation took approximately 8 minutes. As a reference, the same simulation using MathCAD takes approximately 5 hours to complete.

6. CONCLUSION AND FUTURE WORK

We have shown that determining the appropriate optical propagation technique for optical MEM systems is non-trivial. The common propagation methods, Ray, Gauss, and Fraunhofer (far field), used in standard optical CAD tools are not appropriate for OMEM systems. For OMEM systems, the optical propagation method must be more rigorous, to accurately model the small sizes and distances of propagation used in these systems.

Future modeling efforts will be focused on explicitly modeling the fiber/free-space interface and modeling non-uniform effects, such as surface deformities from fabrication or components with curvatures in their surfaces. The scattering effects of these surfaces is of interest. For components with "substantial" curvatures, the scalar Fresnel-Kirchoff formulation will have to also be used instead of our current Rayleigh-Sommerfeld model.

ACKNOWLEDGMENTS

We would like to acknowledge the support of DARPA contract number F3602-97-2-0122 and NSF grant ECS-9616879.

REFERENCES

1. Abramowitz, M. and Stegun, I. A., editors, *Handbook of Mathematical Functions with Formulas, Graphs, and Mathematical Tables*, (Dover Publications, Inc., New York, 1972).
2. Born, M., Wolf, E., *Principles of Optics*, 7th Edition, (Cambridge University Press, 1999).
3. Buck, J., Ha, S., Lee, E.A., Messerschmitt, D., "Ptolemy: a framework for simulating and prototyping heterogeneous systems," *Int. J. Computer Simulation*, Vol. 4, 1994, pp. 155-182.
4. Goodman, J.W., *Introduction to Fourier Optics*, Second Edition (The McGraw-Hill Companies, Inc., 1996).
5. Hecht, E., *Optics*, Second Edition (Addison-Wesley Publishing Company, 1987).
6. Hornbeck, L.J., "Digital Light Processing™: A New MEMS-Based Display Technology," http://www.ti.com/
7. Kurzweg, T.P., Levitan, S.P., Marchand, P.J., Martinez, J.A., Prough, K.R., Chiarulli, D.M., "CAD for Optical MEMS," *Proceedings of the 1999 Design Automation Conference*, New Orleans, LA, June 20-25, 1999, pp.879-884.
8. Lee, S.S., Motamedi, E., Wu, M.C., "Surface-micromachined free-space fiber optic switches with integrated microactuators for optical fiber communication systems," in *Proceedings of the 1997 International Conference of Solid-State Sensors and Actuators (TRANSDUCERS 97)*, 1997, paper 1A4.07P.
9. Levitan, S.P., Kurzweg, T.P., Marchand, P.J., Rempel, M.A., Chiarulli, D.M., Martinez, J.A, Bridgen, J.M., Fan, C., McCormick, F.B., "Chatoyant: a computer-aided design tool for free-space optoelectronic systems," *Applied Optics*, Vol. 37, No. 26, September, 1998, pp. 6078-6092.
10. Levitan, S.P., Marchand, P.J., Kurzweg, T.P., Rempel, M.A., Chiarulli, D.M., Fan C., McCormick, F.B., "Computer-Aided Design of Free-Space Opto-Electronic Systems," *Proceedings of the 1997 Design Automation Conference*, Anaheim, CA, June 1997, Best Paper Award, pp. 768-773.
11. Lin, L.Y., Goldstein, E.L., Tkach, R.W., "Free-Space Micromachined Optical Switches with Submillisecond Switching Time for Large-Scale Optical Crossconnects," *IEEE Phot. Technology Letters*, Vol. 10, No.4, April 1998, pp. 525-527.
12. Marxer, C., de Rooij, N.F., "Micro-Opto-Mechanical 2x2 Switch for Single-Model Fibers Based on Plasma-Etched Silicon Mirror and Electrostatic Actuation," *Journal of Lightwave Technology*, Vol. 17, No. 1, January 1999, pp. 2-6.
13. MEMSCAP, http://memscap.e-sip.com/
14. Microcosm Technologies, http://www.memcad.com/
15. Mukherjee, T., Fedder, G.K., "Structured Design Of Microelectromechanical Systems," *Proceedings of 34th Design Automation Conference Anaheim, CA,* June 1997, pp. 680-685.
16. Optical Micro-Machines Inc, http://www.omminc.com/
17. Optiwave Corp., http://www.optiwave.com/
18. RSoft, Inc., http://www.rsoftinc.com/
19. Saleh, B.E.A., Teich, M.C., *Fundamentals of Photonics* (New York: Wiley-Interscience, 1991).
20. "'Seesaw' Switch is First Practical Micro-Electro-Mechanical Optical Switch," http://www.bell-labs.com/news/1999/february/23/1.html.
21. Wu, M.C., "Micromachining for optical and Optoelectronic Systems," *Proceedings of the IEEE*, Vol. 85, No. 11, (November 1997), pp. 1833-1856.